Aberrant Whole-Brain Resting-State Functional Connectivity Architecture in Obsessive-Compulsive Disorder: An EEG Study

Bo Tan, Jing Yan, Junjun Zhang, Zhenlan Jin, and Ling Li

***Abstract*—Obsessive-compulsive disorder (OCD) is a common neuropsychiatric disorder characterized by intrusive thoughts (obsessions) and repetitive behaviors (compulsions), and few studies have assessed the whole-brain functional connectivity architecture of OCD with electroencephalogram (EEG) during different resting states. Graph theory and network-based statistics (NBS) were employed to examine the neural synchronization and the whole-brain functional connectivity (FC) based on the phase-locking value (*PLV*) of OCD patients and healthy controls (HCs) during eyes-closed (EC) and eyes-open (EO) states. Compared with HCs, OCD patients exhibited not only decreased global synchronization in terms of phase synchrony but also aberrant global topological properties (decreased average shortest path lengths and normalized shortest path lengths together with increased global efficiencies and normalized clustering coefficients) together with inhibited intrahemispheric and interhemispheric FCs during rest, which suggested an imbalance between functional integration and segregation of brain networks for OCD patients. Meanwhile, OCD patients had increased global efficiencies and normalized clustering coefficients, but decreased average clustering coefficients and normalized shortest path lengths together with significantly decreased FCs in the alpha band from EC to EO states, which suggested a dynamic switch between highly integrated (EC state) and highly specialized (EO state) modes of information processing. Moreover, the decreased FCs of OCD patients showed obvious hemispheric asymmetry within or between groups during EC and EO states, which might serve as a potential biomarker to classify OCD patients from HCs.**

***Index Terms*—Obsessive-compulsive disorder, brain functional connectivity, phase-locking value, network-based statistics, resting-state.**

Manuscript received 7 April 2022; revised 2 June 2022; accepted 28 June 2022. Date of publication 4 July 2022; date of current version 15 July 2022. This work was supported in part by the National Natural Science Foundation of China under Grant 61773092 and Grant 62176045 and in part by the Program of Introducing Talents of Discipline to Universities through the 111 Project under Grant B12027. *(Corresponding author: Ling Li.)*

This work involved human subjects or animals in its research. The authors confirm that all human/animal subject research procedures and protocols are exempt from review board approval.

The authors are with the Key Laboratory for NeuroInformation of Ministry of Education and the High-Field Magnetic Resonance Brain Imaging Key Laboratory of Sichuan Province, Center for Information in Medicine, School of Life Science and Technology, University of Electronic Science and Technology of China, Chengdu 610054, China (e-mail: botan@uestc.edu.cn; jiaodayanjing@swjtu.edu.cn; jjzhang@uestc.edu.cn; jinzl@uestc.edu.cn; liling@uestc.edu.cn).

This article has supplementary downloadable material available at https://doi.org/10.1109/TNSRE.2022.3187966, provided by the authors.

Digital Object Identifier 10.1109/TNSRE.2022.3187966

I. Introduction

OBSESSIVE-compulsive disorder (OCD) is a recurrent and refractory chronic mental disorder with high morbidity, which is characterized by unwanted and intrusive thoughts or images (obsessions) and excessive ritualistic behaviors or mental acts (compulsions) typically performed in response to the obsessions [1], [2]. OCD would not only seriously damage individual mental activity in cognitive, emotional, and behavioral aspects, but also affect patients' social functions such as learning and work, which would add a heavy economic burden on society [1], [2]. Most of the early studies have suggested that the pathophysiology of OCD was associated with the dysfunctional cortico-striato-thalamo-cortical (CSTC) loop, which was a widely accepted neurobiological model of OCD [2], [3]. CSTC loop worked by projecting signals from the cerebral cortex to the striatum, transmitting signals to the thalamus through the globus pallidus, and finally feeding back to the cerebral cortex, mainly in the dorsolateral prefrontal cortex (DLPFC), orbital frontal cortex (OFC), anterior cingulate cortex (ACC), thalamus and sensorimotor loops *et al.* [2], [3]. Although the pathogenesis of OCD has been studied by using different methods from the regional properties of the brain, the underlying neurobiological mechanism remains not yet fully understood from a global perspective of the brain at present [3]. The understanding of the aberrant global topological organization and information processing was valuable to providing the advancement of treatment and prevention strategies.

Previous studies of neuroimaging have observed aberrant FCs among different brain regions in OCD patients [4], [5]. Sakai *et al.* showed significantly increased positive FCs between the bilateral ventral striatum and several brain regions, including OFC, DLPFC, and ventromedial prefrontal cortex (VMPFC) based on Functional Magnetic Resonance Imaging (fMRI) [4]. Li and his colleagues also found significantly increased positive FCs between the regions of interest (ROIs) in the right anterior prefrontal cortex and the insula [5]. However, Zhang *et al.* found OCD patients showed decreased FCs in the posterior temporal regions but increased FCs in various control regions such as the cingulate, precuneus, thalamus, and cerebellum, which exhibited aberrant small-world architecture of top-down control networks compared with HCs [6]. Meanwhile, another study also suggested that OCD patients exhibited disruptions in small-world properties of the orbitofronto-striato-thalamic circuit (OFST), and decreased FCs between the central orbitofrontal cortex and dorsomedial striatum but increased FCs between the medial thalamus and striatal areas, which further indicates an imbalance between functional integration and segregation of the brain [7]. Although previous neuroimaging studies have revealed neurobiological abnormalities in OCD patients, the consensus of these findings was still elusive. Recently, a growing body of evidence consistently showed that OCD might derive from distortions within large-scale brain networks rather than abnormal individual subnetworks in specific ROIs by seed-based approaches [6]–[9]. After all, the selected ROIs were usually based on a priori anatomical considerations with the hypothesis of local abnormalities [10], [11] or task-based symptom provocation paradigm [12], [13] in previous studies. Few studies have looked at the topological organization of the whole-brain in OCD patients in different resting states. Furthermore, fMRI with low temporal resolutions could not reveal the sub-second time precision required by the neural mechanism of integrating and coordinating processing between different regions, such as modulating interactions among neurons and regulating information communication [14], [15].

Except neuroimaging, electroencephalogram (EEG) and magnetoencephalogram (MEG) with high temporal resolution were also used to explore the brain abnormalities of OCD patients by defining interactions among different brain regions. The most consistent findings were topographic abnormalities in the frontal and orbitofrontal areas detected by EEG or MEG [16]–[18]. For example, Velikova *et al.* showed that OCD patients had increased current density for delta in the insula and beta in the frontal, parietal, and limbic lobes, while decreased inter-hemispheric coherence and reduced coupling between delta and beta bands [17]. Another study of OCD also found decreased interhemispheric coherence and lagged non-linear coherence between frontal brain areas during rest, including the anterior cingulate cortex, the superior frontal gyrus, and the left medial frontal gyrus [19]. Although these results were inconsistent regarding the abnormalities of specific EEG frequency bands and showed both decreases and increases of low-frequency (delta and theta bands) as well as fast-frequency (alpha and beta bands) activities [19], [20], multiple frequency bands of brain activity were indeed closely associated with the brain abnormalities of OCD patients, which was also supported by the studies of resting-state MEG based on inter-regional phase synchrony among the OFC, insula, and cortical regions of the limbic lobe [21]. And then, the study of whole-brain functional networks in different frequency bands would promote our understanding of the alterations of brain dynamics and topological properties of OCD patients from a global perspective based on resting-state EEG.

Based on the previous findings of neuroimaging and neuro-electrophysiology, the aim of the current study is to evaluate whether whole-brain functional networks of OCD patients are aberrant in different frequency bands during different resting states. Here, the *PLV* was used for measuring the phase synchrony between channel pairs to construct FCs, which was particularly suitable for connectivity analysis by providing measurements of neural signal temporal relationships and regardless of their signal amplitude [21], [22]. Furthermore, resting-state EEGs were acquired during EC and EO states, which were fundamental behaviors for directing attention to the external and the internal world [23], [24]. After constructing matrices of phase synchrony by using the *PLVs*, graph theoretical analysis and the whole-brain Network-Based Statistic (NBS) were applied to analyze the synchronization and topological properties of the whole-brain functional networks (including topological parameters (such as network efficiencies, small-world properties) and topological connectivity) during EC and EO states. Moreover, based on the above analysis model, we further investigated the alteration of brain functional networks from EC to EO states to reveal the difference of the topological organization and information processing in OCD patients during different resting states.

II. Materials and Methods

A. Participants

The participants were composed of 17 right-handed OCD patients and 17 right-handed HCs, recruited from the Sleep Health Center, West China Hospital, Sichuan University, Chengdu, China. All participants were diagnosed by two experienced psychiatrists according to the Diagnostic and Statistical Manual of Mental Disorders (DSM-IV). All participants with a history of clinically important head injuries, alcohol or drug abuse, mental retardation, family or personal history of mental illness, and auditory or visual impairment seizures or neurological diseases were excluded. Part of OCD patients (13/17) were medicated before collecting EEG data. The Obsessive-Compulsive Inventory-Revised (OCI-R) and the Yale-Brown Compulsive Scale (Y-BOCS) were used for assessing the severity of obsessive-compulsive symptoms. In addition, the Wechsler Adult Intelligence Scale (WAIS-RC: mainly including information (I), similarities (S), vocabulary (V), picture completion (PC), block design (BD), and picture arrangement (PA)) was used for assessing the total intelligence level of OCD patients and HCs. Beck Depression Inventory (BDI, 13 items) and Beck Anxiety Inventory (BAI, 21 items) were used for assessing the degree of depression and anxiety of OCD patients and HCs respectively.

The study was approved by the institutional ethical review board of West China Hospital, Sichuan University, and all participants provided their signed written informed consent before participation in this study.

B. EEG Acquisition and Data Preprocessing

All EEG data were recorded by a 64 Brain Cap MR (Brain Product, Germany). The electrical sampling rate was 500 Hz, and the channel impedance was lower than 10 kΩ. The reference channel was the FCz. The resting-state recording consisted of a three-minute EC conditions followed by a three-minute EO conditions. Firstly, all participants were required to relax and remain awake when EEG data were collected for three minutes during the EC state. Then participants were required to open their eyes and simply gaze at the cross in the middle of the front screen for three minutes. The EEG data of each participant was recorded for six minutes. Finally, all participants got the corresponding remuneration after finishing all experiments.

The recorded EEG data might be affected by artifacts (eye blinks, eye movements, scalp or heart muscle activity, line or other environmental noise). Independent Component Analysis (ICA) was used to remove some of these artifacts (mainly electrocardiogram (ECG) or electrooculogram (EOG) artifacts, etc.) from EEG data. The malfunctioning signals were replaced with the interpolated values from the neighboring channels. After eliminating the influence of various artifacts, the 30s artifact-free EEG data (15000 sample points) were selected from each participant and divided into five segments. Each segment of the EEGs was decomposed into the conventional EEG frequency bands, including theta (4-7 Hz), alpha (8-12 Hz), beta (13-30 Hz), and gamma (31-48 Hz) bands for calculating *PLVs*. To further improve the reliability of the current results, we took the average *PLVs* of the five segments in each frequency band and applied them in the subsequent analysis of brain functional networks. Furthermore, the filtered EEG data were processed by the current source density (CSD) toolbox to minimize the contribution of volume conduction and remove spurious synchronization, which was supplied by Kayser and Tenke [25], [26].

C. Measures of Whole-Brain Functional Networks

1) The Interaction of Phase-Locking Value: Synchronous oscillation is a universal phenomenon in the nervous system, which is important for the understanding of information-processing mechanisms in the brain [27], [28]. The synchronization analysis of EEG can help better understand the cognitive function of the brain [28]. As a fundamental and common neuronal mechanism, the phase synchrony among EEG signals could effectively distinguish cognitive functions of different conscious tasks/responses in humans, which was characterized by ignoring the influence of amplitude and only relying on the instantaneous phase of EEG signals to detect the weak correlation between different signals [27], [29]. To characterize the value of phase synchrony, Lachaux *et al.* proposed the *PLV* to describe the correlation of phase synchrony between two-time series [28], which was an effective method to measure the phase synchrony of the brain. The *PLV* could reflect the overall "tendency" of the phase difference between two real signals and could effectively separate the phase components of EEG signals, which had been applied to study brain functional networks under different conditions [28]. The conventional implementation method of *PLV* was to decompose EEG signals into instantaneous amplitude and instantaneous phase by the Hilbert transform and then calculate the correlation between the instantaneous phases of the different signals [28], [29]. The level of synchronization between different EEG signals was often measured by employing 1:1 phase synchrony in the brain. The calculation method of the *PLV* was defined as:

$$PLV = \left| \frac{1}{N} \sum_{n=1}^{N} \exp(i\,[\phi_1(n) - \phi_2(n)]) \right|$$

where N was the length of time series. $\phi_1(n)$ and $\phi_2(n)$ were the instantaneous phase of two signals at time point n respectively. The formula took the means of phase angle differences between two signals over time. The *PLV* was an excellent technique to estimate the strength and significance of instantaneous phase coupling between two EEG signals [28]. The *PLVs* ranged from "zero" to "one". A value of "zero" indicated that no coupling occurs, while a value of "one" indicated perfect phase locking [28], [29]. In this paper, the *PLVs* was used to measure the FCs of OCD patients and HCs between all channel pairs (regions) during rest.

2) Graph Theoretical Analysis: The brain is a complex network with the characteristics of an economical small-world network, and graph theory can help understand better the topological properties of the large networks [30], [31]. The *PLV* generated a value of connectivity strength for each channel pair to construct matrices of phase synchrony in each frequency band. And then the matrices of phase synchrony were converted into binary matrices (the matrices of FCs) with the thresholding based on the sparsity of networks in this study (the sparsity was defined as the ratio of the number of existing edges divided by the maximum possible number of edges in a network) [30], [32]. And then the matrices of FCs could be visualized by a graph where the nodes correspond to EEG channels and undirected edges corresponded to the *PLVs* which were above the thresholds. The thresholds ranged from 0.10 to 0.50 (with an interval of 0.05) for the subsequent analyses. Finally, several characteristic topological parameters were investigated to characterize the topological performance of brain functional networks in OCD patients and HCs, including average clustering coefficients, average shortest path lengths, global efficiencies, local efficiencies, normalized clustering coefficients, and normalized shortest path lengths [31], [32].

3) The Distribution of Functional Hubs: The centrality of a node indicated the importance of its function, and the high centrality of nodes would serve as the centers of information integration [21], [33]. Since the *PLV* could better measure the neuronal interaction between two brain regions, the nodal degree (*Dnodal*) was calculated by the total *PLV* of the nodes which were connected to a given node to characterize the centrality of a node in brain functional networks [21]. The greater *Dnodal* of a node, the more important the node was in a network. For each subject, the top 5% nodes of which the *Dnodal* values were ranked were considered in the hub calculation [21]. To examine the different distribution of important nodes of OCD patients and HCs, we evaluated the aggregated ranking percentage across all participants and determined the top 10% of *Dnodal* nodes in each frequency band as the characteristics of the group [21]. Finally, several functional nodes with high centrality of brain functional networks were detected in OCD patients and HCs respectively, which were projected into the topological brain map in each frequency band.

4) Network-Based Statistic: To identify the hyper and hypo-connected components in OCD patients, the matrices of the whole-brain *PLVs* were examined to extract subnetworks or topological clusters that were significantly different between OCD patients and HCs by using the whole-brain NBS [34]. NBS was a nonparametric statistical method to deal with the multiple comparison problem in conducting mass univariate significance testing among graphs. Compared with other statistical methods of a network, NBS could estimate family-wise error (*FWE*) correction for associations pairs between nodes, and was sensitive to detecting distributed networks with multiple connections [34], [35]. This method was previously used to investigate the neurological basis of other psychotic disorders, such as depression, schizophrenia, etc. [35], [36]. Therefore, NBS was selected to analyze the different connected components of brain functional networks of OCD patients and HCs in this study.

In the comparative analysis, we tested the hypotheses of hyper-connectivity ("OCD > HC") and hypo-connectivity ("OCD < HC") between OCD patients and HCs. Firstly, the statistical difference of each FC was calculated by a two-sample *t-test* between OCD patients and HCs. After comparing the test results with a pre-specified statistical threshold T, the connections above the exclusion threshold were included in a set of "hyper-threshold connections". And then permutation tests were applied to ascribe a p-value controlled for the family-wise error rates (*FWER*) to each connected component in terms of its size [34], [36]. For each permutation, the test statistics of connected components were recalculated after defining a set of suprathreshold connections above the same threshold. The maximal connected component in the set of suprathreshold connections derived from each of multiple permutations was then determined and was sensitive to the significantly different FCs between OCD patients and HCs. The p-value of an observed component was estimated by finding out the total number of permutations to identify the maximal component size [34]. Visualization of significant components between networks was conducted using BrainNet Viewer V1.53 [37].

D. Statistical Analysis

The NBS performed a two-dimension comparison of OCD patients and HCs in the study. The contrasts were set as "OCD < HC" and "OCD > HC" between groups or "EC < EO" and "EC > EO" in OCD patients. The *FWER* was controlled at cluster level with $p < 0.05$. The number of permutations was 5000, and the statistic threshold was set as $T \geq 3.0$. The two-sample *t-test* was applied to test the difference of topological parameters between OCD patients and HCs. Statistical significance was set at $p < 0.05$, corrected for multiple comparison by false discovery rate (*FDR*). The demographic and clinical characteristics of the two groups were conducted with two-sample *t-tests* or a χ^2 test. $p < 0.05$ was applied as significance in all tests. All operations were done in Matrix Laboratory (MATLAB v7.14) (MathWorks, Inc, Sherborn, MA). The statistical procedures were completed in Statistical Product and Service Solutions (SPSS v20.0) (SPSS, Chicago, IL, USA).

III. Results

A. Demographic and Clinical Data

The demographic and clinical characteristics of all participants were given in Supplementary TABLE SI. All 34 subjects participated in the study, including 17 OCD patients (male/female, 7/10) and 17 age- and sex-matched HCs (male/female, 8/9). The OCD patients had a mean age of 29.31 $\pm$ 4.26 and a mean education of 14.55 $\pm$ 2.75 years. The HCs had a mean age of 29.13 $\pm$ 6.71 years and a mean education of 15.23 $\pm$ 4.07. There was no significant difference between OCD patients and HCs in terms of age, gender, or education level. Meanwhile, the significant difference between OCD patients and HCs in the total intelligence quotient (IQ) (OCD patients: 110.97$\pm$12.52, HCs: 105.43$\pm$14.95, $p = 0.085$) was not found. However, the mean Y-BOCS total score of OCD patients was significantly higher than that of HCs in the OCI-R scale ($p < 0.05$), BAI scale ($p < 0.05$), and BAD scale ($p < 0.05$).

B. Comparison of Synchronization and Functional Hubs of OCD Patients and HCs During Rest

To find out the difference of the *PLV* matrices between OCD patients and HCs, the mean of *PLVs* was calculated for each channel (the mean of each group) and individual participant (the mean of all channels) respectively in each frequency band during EC and EO states. Compared with HCs, Figure 1a and b showed that OCD patients appeared a decreasing trend of phase synchrony between channel pairs for different frequency bands and different states, especially in the alpha band (the redder the color, the less phase synchrony in OCD patients). Moreover, Figure 1c and d showed that the overall distribution of individual OCD patient was relatively more dispersed and slightly lower the *PLVs* than that of HCs in terms of phase synchrony, while only significant difference between OCD patients and HCs in the alpha band during EC and EO states.

Meanwhile, Figure 1e and f showed partially overlapped functional hubs of OCD patients and HCs, which relatively concentrated in the parietal-occipital region during the EC state, while less overlapped functional hubs were separately dispersed in different regions during the EO state. Compared with HCs, the functional hubs of OCD patients were much closer in the frontal-central regions in the theta band and in the parietal-occipital regions in the beta band. Moreover, the distribution of functional hubs of both OCD patients and HCs displayed obvious hemispheric asymmetry, with more functional hubs in the right hemisphere than that in the left hemisphere in alpha and beta bands.

C. Comparison of Topological Parameters of OCD Patients and HCs During Rest

Based on the constructed weighted matrices of the *PLVs*, several topological parameters of binary networks after the thresholds were calculated to describe the topological properties of brain functional networks in different frequency bands.

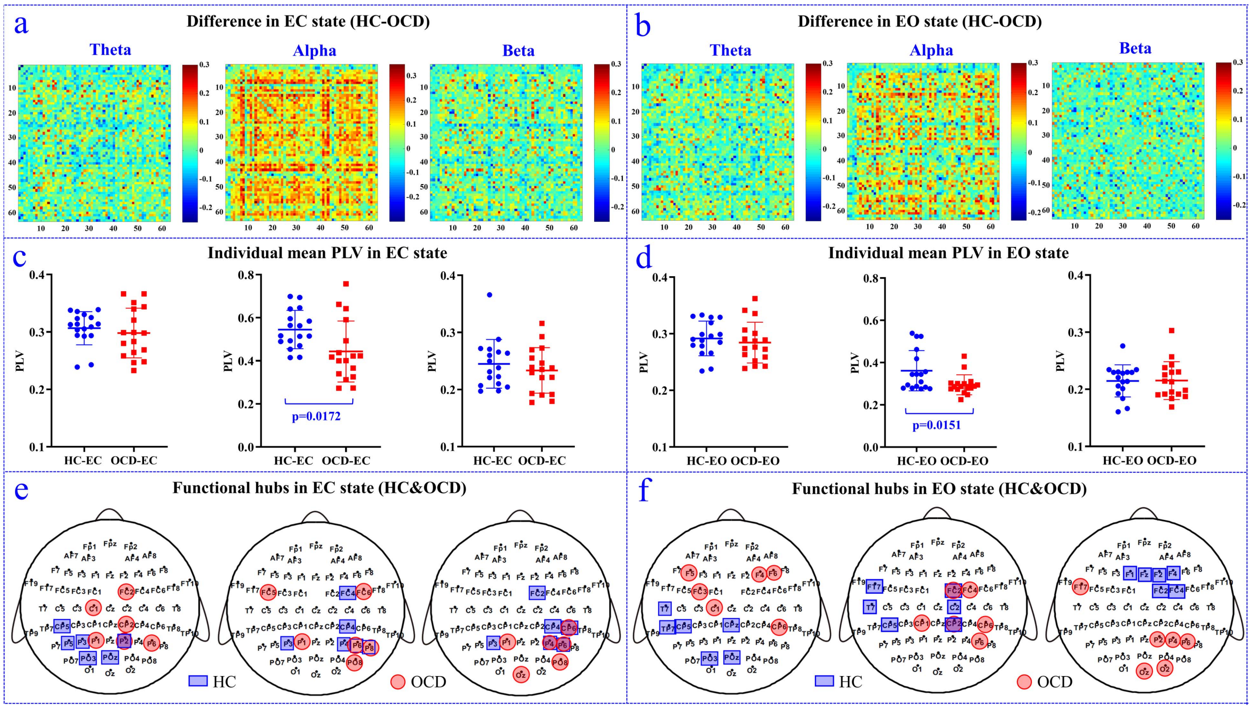

Fig. 1. The difference of phase-locking values (*PLVs*) and functional hubs of OCD patients and HCs in theta, alpha, and beta bands during EC and EO states. Fig.1a and b respectively represent the difference of mean *PLVs* in full connectivity matrices between groups during EC and EO states (HC minus OCD patients). Fig.1c and d depict scatter plots of the mean *PLVs* of the individual participant during EC and EO states. Fig.1e and f display the distribution of functional hubs of OCD patients and HCs during EC and EO states. Each column exhibits the results of each frequency band during each resting state. The color bar depicts the difference of the average *PLVs* between OCD patients and HCs (HC - OCD). The red translucent circles and the blue translucent squares represent the functional hubs of OCD patients and HCs respectively. OCD: obsessive-compulsive disorder; HC: healthy control; EC: eyes-closed; EO: eyes-open.

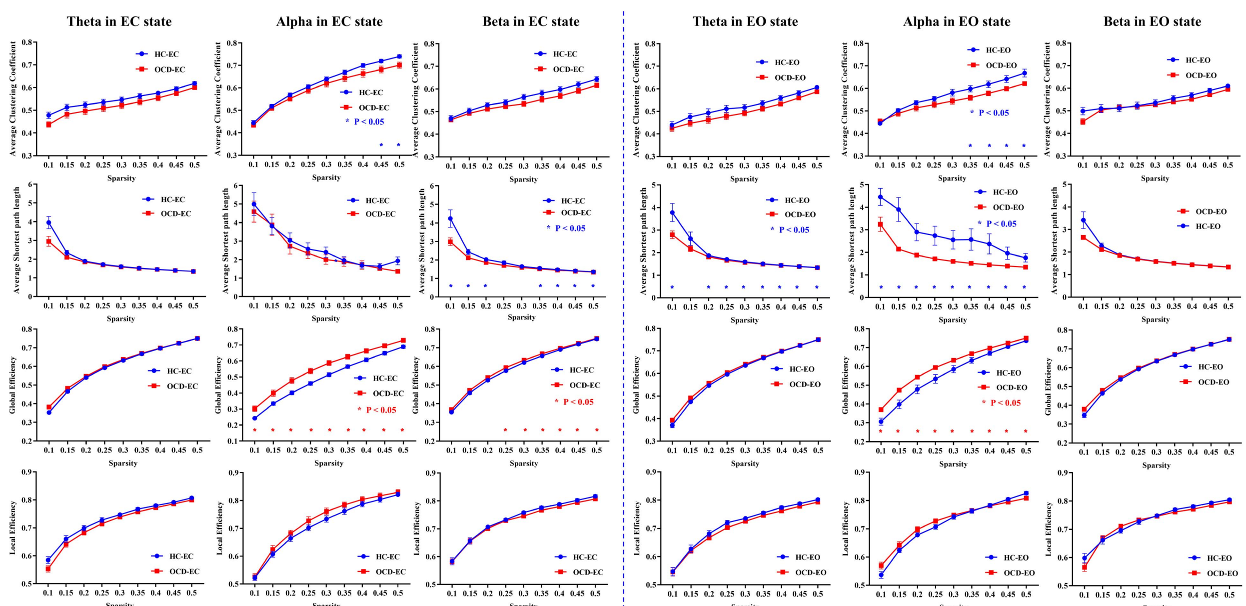

Fig. 2. The topological parameters of whole-brain functional networks of OCD patients and HCs in theta, alpha, and beta bands during EC and EO states, including average clustering coefficients, average shortest path lengths, global efficiencies, and local efficiencies. The red asterisks indicate that the topological parameters of OCD patients are significantly higher than that of HCs, and the blue asterisks indicate that the topological parameters of OCD patients are significantly lower than that of HCs ($*p < 0.05$, FDR corrected). Standard errors of the mean (SEM) are shown with error bars. OCD: obsessive-compulsive disorder; HC: healthy control; EC: eyes-closed; EO: eyes-open.

Figure 2 consistently showed that there were some aberrant topological parameters of OCD patients during both EC and EO states. Compared with HCs during the EC state, the global efficiencies of OCD patients significantly increased in alpha and beta bands, while the average shortest path lengths decreased only in the beta band. Similarly, compared

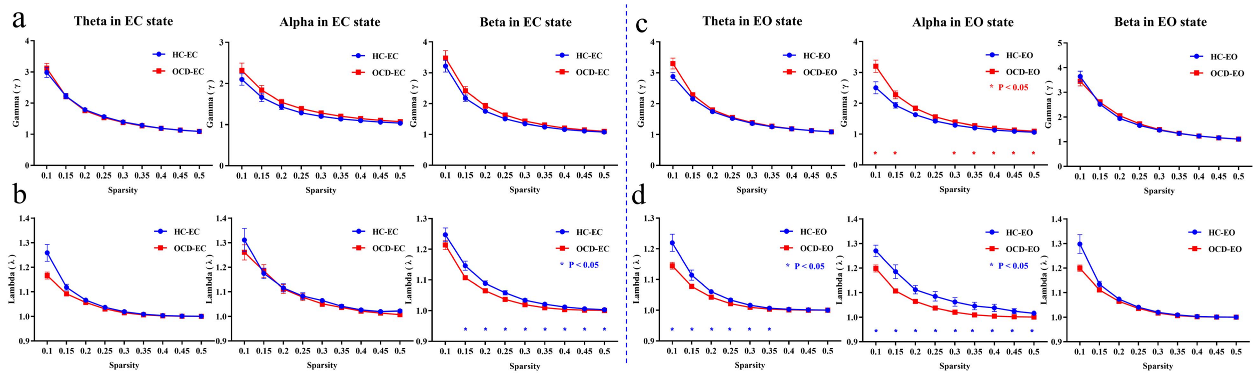

Fig. 3. The small-world parameters of whole-brain functional networks of OCD patients and HCs in theta, alpha, and beta bands. The left panel displays small-world parameters of the EC state, and the right panel displays small-world parameters of the EO state, including normalized clustering coefficients(γ), and normalized shortest path lengths(λ). The red asterisks indicate that the small-world parameters of OCD patients were significantly higher than that of HCs, and the blue asterisks indicate that the small-world parameters of OCD patients were significantly lower than that of HCs ($^*p < 0.05$, FDR corrected). Standard errors of the mean (SEM) were shown with error bars. OCD: obsessive-compulsive disorder; HC: healthy control; EC: eyes-closed; EO: eyes-open.

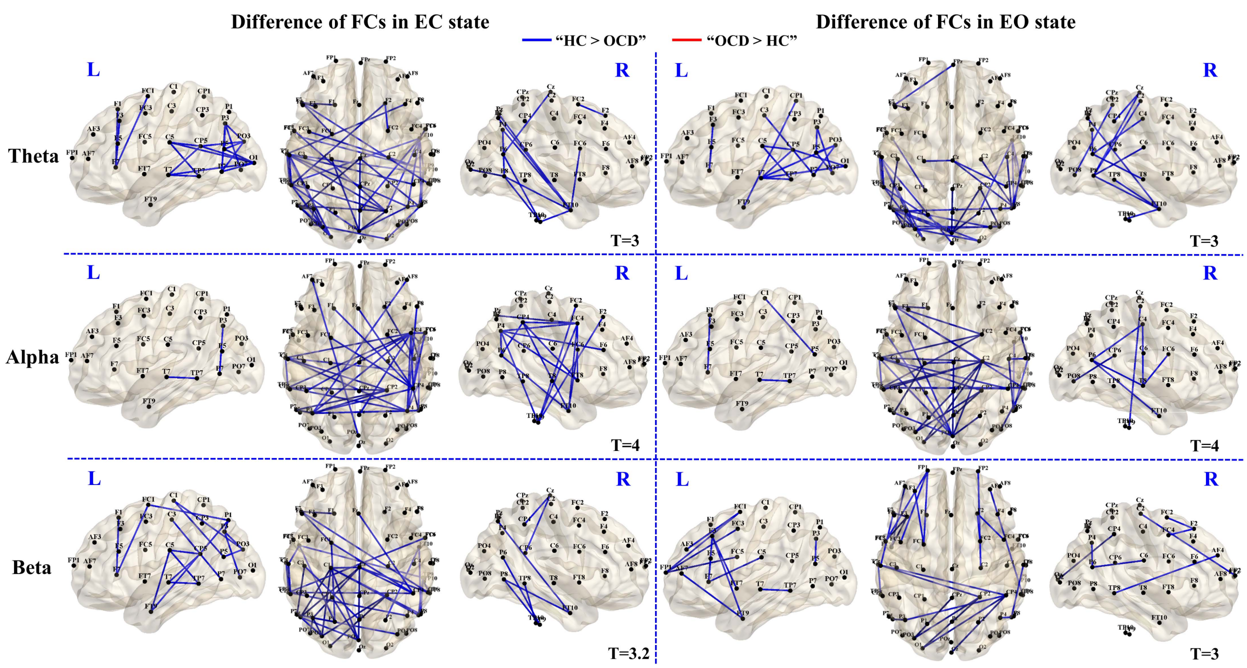

Fig. 4. The difference of brain functional networks between OCD patients and HCs by using the whole-brain network-based statistics (NBS) during EC and EO states. The identified subnetworks (connected components) represent the difference of FCs between OCD patients and HCs based on the *PLVs* in theta, alpha, and beta bands. The blue lines represent the FCs of "HC > OCD", and the red lines represent the FCs of "HC < OCD" in the brain model. Left panel displays significantly decreased FCs of OCD patients compared with HCs ("HC > OCD") during the EC state ($p < 0.05$, FWE-corrected). Right panel displays significantly decreased FCs of OCD patients compared with HCs ("HC > OCD") during the EO state ($p < 0.05$, FWE-corrected). Representations are obtained with the BrainNet Viewer Toolbox [37].

with HCs during the EO state, the global efficiencies of OCD patients significantly increased only in the alpha band, while the average shortest path lengths decreased in theta and alpha bands. Furthermore, in the alpha band, the average clustering coefficients of OCD patients were also lower than those of HCs during both EC and EO states under partial sparsity.

Moreover, Figure 3 displayed that both OCD patients and HCs exhibited small-world architectures under the thresholds, which were characterized by more locally clustered ($\gamma > 1$) and an almost identical path length ($\lambda \approx 1$) in comparison with the matched random networks in each frequency band. However, compared with HCs, the normalized clustering coefficients(γ) of OCD patients significantly increased in the alpha band during the EO state, while normalized shortest path lengths decreased in the beta band during the EC state and in both theta and alpha bands during the EO state. No significant group differences of topological parameters between OCD patients and HCs were observed in the gamma band.

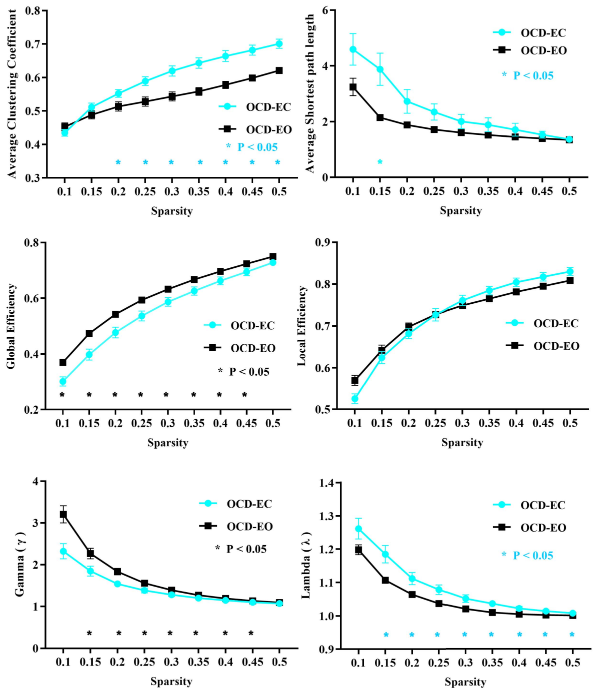

Fig. 5. The alteration of topological parameters of brain functional networks in OCD patients from EC to EO states in the alpha band, including average clustering coefficients, average shortest path lengths, global efficiencies, local efficiencies, normalized clustering coefficients(γ) and normalized shortest path lengths(λ). Standard errors of the mean (SEM) are shown with error bars. The turquoise asterisks indicate that the topological parameters of the EC state are significantly higher than those of the EO state, and the black asterisks indicate that the topological parameters of the EC state are significantly lower than those of the EO state (*$p < 0.05$, *FDR* corrected). OCD: obsessive-compulsive disorder; eyes-closed (EC); eyes-open (EO).

D. Comparison of FCs of OCD Patients and HCs During Rest

Group differences of FCs between OCD patients and HCs were also explored by using whole-brain NBS during rest. NBS analysis only found the contrast of "HC > OCD", which revealed the inhibited resting-state whole-brain connectivity architecture of OCD patients in different frequency bands, consisting of intra-hemispheric and interhemispheric FCs in Figure 4. Compared with HCs during EC and EO states, the FCs of OCD patients in theta and alpha bands decreased significantly in the central and parietal-occipital regions. However, the FCs of OCD patients only in the beta band decreased in the left frontal regions during the EO state.

Furthermore, the decreased FCs of OCD patients also showed obvious hemispheric asymmetry in the alpha band which showed more decreased FCs in the right hemisphere than that in the left hemisphere, while the decreased FCs were distributed in both hemispheres in theta and beta bands. Meanwhile, compared with HCs, some long-rang connections of OCD patients between the left and right hemispheres were also significantly decreased in each frequency band during rest. There were more inhibited FCs of the EC state than those of the EO state. Notably, these results consistently suggested that brain functional networks of OCD patients were indeed inhibited during rest, yet there were some differences in the

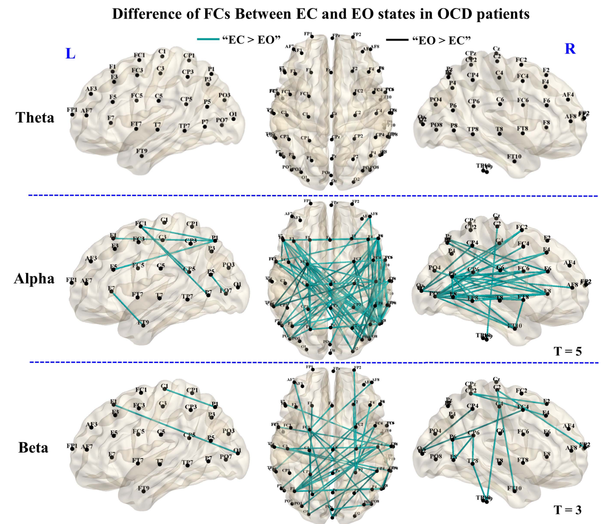

Fig. 6. The alteration of brain functional networks in OCD patients from EC to EO states by using the whole-brain Network-Based Statistics (NBS). The identified subnetworks (connected components) represent the difference of FCs between OCD patients, and HCs based on the *PLVs* in theta, alpha, and beta bands. The turquoise lines represent the FCs of "EC > EO" and the black lines represent the FCs of "EO > EC" in the brain model ($p < 0.05$, FWE-corrected). Each row displays the results of NBS in each frequency band. Representations are obtained with the BrainNet Viewer Toolbox [37].

distribution of nodes and connections between EC and EO states. No significantly different network components of brain functional networks were derived from the contrasts of "OCD < HC" or "OCD > HC" in the gamma band and the contrast of "OCD > HC" in theta, alpha, and beta bands.

E. The Alteration of Brain Functional Networks of OCD Patients From EC to EO States

The alteration of brain functional networks was further investigated from EC to EO states in terms of topological parameters and FCs in OCD patients. Figure 5 showed that the alteration of topology parameters from EC to EO states was also mainly concentrated in the alpha band, involving increased global efficiencies and normalized clustering coefficients (γ), decreased average clustering coefficients and normalized shortest path lengths (λ). No significantly different topological parameters between EC and EO states with OCD patients were observed in the gamma band.

NBS analysis only found the contrast of "EC > EO" from EC to EO states in OCD patients. Figure 6 showed that the significantly decreased FCs of OCD patients in the central and parietal-occipital regions from EC to EO states in alpha and beta bands, especially interhemispheric and the right intra-hemispheric long-rang FCs in the alpha band, which also suggested obvious hemispheric asymmetry of decreased FCs in OCD patients from EC to EO states. No significantly different network components of brain functional networks were found in the contrasts of "EC < EO" or "EC > EO" in theta and gamma bands.

IV. Discussion

Based on resting-state EEGs (contains EC and EO states), the current study aimed to investigate whether OCD patients showed aberrant brain functional networks in terms of topological parameters and FCs in different frequency bands. Compared with HCs, OCD patients exhibited not only decreased global synchronization but also aberrant global topological properties (some disruptions of topological parameters and small-world properties) together with inhibited intra-hemispheric and interhemispheric FCs during rest, which suggested an imbalance between functional integration and segregation of brain networks for OCD patients. Meanwhile, OCD patients also exhibited significantly decreased FCs in the central and parietal-occipital regions from EC to EO states in alpha and beta bands, especially more decreased in interhemispheric and the right intra-hemispheric long-rang FCs in the alpha band. Moreover, the decreased FCs of OCD patients showed obvious hemispheric asymmetry within or between groups during EC and EO states, which might serve as a potential biomarker to classify OCD patients from HCs.

A. Aberrant Topological Parameters of Whole-Brain Functional Networks in OCD Patients During Rest

The human brain is a dynamically interconnected functional system with economical small-world architecture, which has an optimal balance between local specialization and global integration [38], [39]. Numerous studies have shown that topological parameters of a network were closely related to cognitive functions such as working memory and emotion *et al.* [40], [41], and aberrant topological parameters have been found in many neuropsychiatric disorders [6], [42]. Similarly, compared with HCs, some aberrant topological parameters of OCD patients have been found in the current study, including average clustering coefficients, average shortest path lengths, global efficiencies, and small-world parameters, especially in the alpha band.

Average shortest path length and global efficiency measure the global transmission capacity between different nodes (regions) in a network, which are comprehensive indexes for the parallel information processing capabilities [43], [44]. Significantly decreased average shortest path lengths together with increased global efficiencies suggested a stronger and overconnected long-range brain structural connectivity, which might lead to the enhancement of remote information integration and transmission capacity in OCD patients. Previous studies have reported that decreased FCs of OCD patients in control networks would lead to the restriction of information transmission among specific brain regions [6], while the whole-brain networks might be over-expressed to cause a higher efficiency and lower cost of information transmission due to the existence of compensation mechanism, which might also be associated with the intrusive thoughts and uncontrollable repetitive behaviors [45]. The above aberrant topological parameters also were further mutually confirmed by the results of different network components between OCD patients and HCs, which was consistent with the previous study based on Diffusion Tensor Imaging (DTI) in OCD patients [45].

The current study found that the brain functional networks of both OCD patients and HCs displayed small-world architectures together with high clustering coefficients and short characteristic path lengths during rest, which were consistent with the results of previous studies [6], [21]. However, compared with HCs, the aberrant small-world properties of OCD patients (significantly increased normalized clustering coefficients together with decreased normalized shortest path lengths) indicated that the optimal allocation of whole-brain topological properties was disrupted to shift toward a more regular organization in the beta band during the EC state and in both theta and alpha bands during the EO state, which may be attributable to a significantly decreased the long-range FCs between two hemispheres to descend signal-propagation speed and synchronizability across distant regions.

B. Aberrant FCs of Whole-Brain Functional Networks in OCD Patients During Rest

The topological properties of a network may be related to the level of synchronization for corresponding rhythms, and oscillations with different rhythms may contribute to different brain functions [46], [47]. The functional hubs and network components were further studied to reveal the differences of brain functional networks between OCD patients and HCs in different frequency bands. Functional hubs of a network were central elements of a network and were highly connected with other regions, and aberrant distribution of functional hubs might affect other connected areas and distributed configuration of FCs. Compared with HCs, functional hubs of OCD patients were closer in the frontal-central regions in the theta band and the parietal-occipital regions in the beta band. Meanwhile, the distribution of functional hubs displayed obvious hemispheric asymmetry (more functional hubs in the right hemisphere than that in the left hemisphere) in alpha and beta bands, which would influence the efficiency of information transmission and processing of the whole-brain functional networks in OCD patients [32]. Meanwhile, hemispheric asymmetry suggested the two hemispheres have their specialized functions to perform information processing in OCD patients [48].

Moreover, compared with HCs, OCD patients showed the inhibited whole-brain resting-state connectivity architecture composed of intra-hemispheric and interhemispheric FCs, which were mainly distributed in the central and parietal-occipital regions in theta and alpha bands. Tracey *et al.* found with fMRI that OCD patients have reduced resting-state FCs from right MTG to left cingulate, bilateral insula, inferior parietal lobule (IPL), and precentral gyrus [48]. Koh *et al.* also have reported the decreased FCs in terms of inter-regional phase synchrony among the OFC, insula, and cortical regions of the limbic lobe, in theta, alpha, beta, and gamma bands using MEG [21]. These results of OCD patients could also further supplement some evidence of decreased FCs by using the whole-brain NBS in different frequency bands. Moreover, previous studies have shown aberrant executive function of OCD patients in terms of inhibitory control and working memory, which were also associated with different rhythms of brain activity [2], [46]. Bazanova *et al.* have suggested that alpha rhythms were associated with multiple cognitive functions such as memory or response inhibition [49], and alpha desynchronization reflected the actual process of cognitive information processing [50]. The significantly decreased phase synchrony and FCs of OCD patients in the alpha band may indicate that OCD patients have stronger alpha desynchronization and weaker synchronization in the cortical or subcutaneous networks than that of HCs. Meanwhile, Zhang *et al.* reported that synchronization and desynchronization in the beta band were closely related to the cognitive process of response inhibition [51]. The significantly decreased FCs of OCD patients may be associated with the impairment of response inhibition in the beta band. In this study, OCD patients showed a decrease in the global synchronization and the whole-brain FCs in multiple frequency bands, which may cause the difficulty of information processing in cognitive functions.

Furthermore, NBS analysis also suggested that the inhibited FCs of OCD patients showed obvious hemispheric asymmetry, with more inhibited FCs in the right hemisphere than that in the left hemisphere, especially in the alpha band. According to Ischebeck et al, OCD patients showed that the altered EEG asymmetry with the frontal alpha power in the 8-10 Hz band was more dominant in the left hemisphere during blocks of rest and presentation of neutral, aversive, and OCD-related pictures [16]. Other studies also found disrupted asymmetry of decrease in interhemispheric and intra-hemispheric FCs within (i.e., orbital frontal cortex and thalamus) and outside (i.e., inferior occipital gyrus and precentral gyrus/postcentral gyrus) the CSTC loop at rest in the pathophysiology of OCD [52], which is further verified by the current findings. Meanwhile, the current results also found that some long-range FCs between two hemispheres were significantly decreased in OCD patients compared with HCs. Based on these findings of previous studies, a well-organized human brain depended on both short-range and long-range FCs, and the lack of long-range FCs would result in inefficient communication [53]. The brain has evolved a balance that optimizes information-processing efficiency across different classes of specialized areas and mechanisms to modulate coupling in support of dynamically changing processing demands [54]. The significantly decreased long-range FCs of OCD patients indicated that the optimal configuration of functional integration and segregation were disrupted in information processing, making it difficult to communicate information among distant regions of the brain. This is additional new evidence for the pathogenesis of OCD [46].

C. Difference of Brain Functional Networks Between EC and EO States in OCD Patients

The resting state usually refers to an eyes-closed (EC) and/or eyes-open (EO) state in EEG, which is a measure of the background or tonic level of brain activity [15], [55]. In the current study, it was further investigated the alteration of brain functional networks from EC to EO states in OCD patients, which was rarely reported in previous studies with EEG. Compared with the EC state, OCD patients showed higher global efficiencies together with normalized clustering coefficients, and lower average clustering coefficients together with normalized shortest path lengths during the EO state, which indicated a decrease in specialized information processing along with an increase in integrated information from EC to EO states [23]. Meanwhile, NBS analysis of OCD patients showed significantly decreased FCs in the central and parietal-occipital regions from EC to EO states in alpha and beta bands, especially more decrease in interhemispheric and the right intra-hemispheric long-rang FCs in the alpha band, which also showed obvious hemispheric asymmetry of decreased FCs and less synchronicity in the brain [52]. Previous studies have shown the average alpha power of occipital regions under the eyes-closed condition was significantly higher than that under the eyes-open condition, which demonstrated the well-established alpha-blocking or alpha desynchronization phenomenon [56], [57]. Other studies also suggested that EC and EO were two different states of mental activity: an "exteroceptive" state characterized by overt attention and ocular motor activity (the EO state) and an "interoceptive" state characterized by imagination and multisensory activity (the EC state) [23], [58]. The decreased FCs of OCD patients are probably derived from an increased attentional load and level of arousal doing with the simple processing of visual information or desynchronization of the whole-brain during the EO state compared with the EC state [58]. These findings further suggested that the topological brain organization would switch dynamically between highly integrated (the EC state) modes and highly specialized (the EO state) modes of information processing as OCD patients open or close their eyes [23]. The current results provided some new evidence of topological differences between EC and EO states, which may be helpful in the diagnosis and treatment of OCD.

D. The Limitation and Expectation

There are several limitations of the current study. Firstly, the low spatial resolution of EEG would affect the accuracy of the channels mapping into exact spatial locations in the brain. The CSD supplied by Kayser and Tenke was applied to decrease this deviation and to compensate for the limited spatial resolution of EEG in the pre-processing of EEG [25], [59]. Other techniques would be used for assessing brain functional networks of OCD patients in the future, such as MEG and fMRI. Secondly, the current study has a relatively small sample size. To improve the reliability of the results in this study, multi-segment EEG time series were extracted to calculate the mean *PLVs* to construct brain functional networks and identify the alteration of FCs in OCD patients. Thirdly, most OCD patients were taking medication at the time of the study, and the confounding effects of these medications cannot be completely excluded. Future studies should be conducted with a larger sample of unmedicated OCD patients. Despite these limitations, the inhibited whole-brain resting-state connectivity architecture also provided valuable insights and new evidence of the aberrant topological characteristics of brain networks for OCD patients during EC and EO states. Moreover, neuroregulatory techniques, such as transcranial magnetic stimulation (TMS) would provide new insights into understanding abnormalities in information processing and topological organization of the whole-brain. Future studies should utilize TMS-EEG to understand the underlying pathophysiology.

V. Conclusion

In conclusion, the current study has proved that the inhibited whole-brain resting-state architecture of OCD patients in the form of decreased global synchronization as well as intra-hemispheric and interhemispheric FCs in different frequency bands during rest. Compared with HCs during EC and EO states, the significantly decreased FCs of OCD patients mainly concentrated in the central and parietal-occipital regions in theta and alpha bands, which indicated an imbalance between functional integration and segregation of brain networks for OCD patients. Moreover, the significantly decreased FCs of OCD patients were also detected in the central and parietal-occipital regions from EC to EO states in alpha and beta bands, particularly more decrease in interhemispheric and the right intra-hemispheric long-rang FCs in the alpha band, which was rarely reported in the previous studies with EEG. The above results also suggested OCD patients have a decrease in specialized information processing together with an increase in integrated information from EC to EO states. Moreover, the obvious hemispheric asymmetry of decreased FCs was observed within or between groups during EC and EO states, which revealed aberrant network patterns and might provide some reference for task states as well as the diagnosis and treatment of OCD in the future.

References

[1] W. K. Goodman, D. E. Grice, K. A. Lapidus, and B. J. Coffey, "Obsessive-compulsive disorder," *Psychiatr. Clin. North Amer.*, vol. 37, no. 3, pp. 67–257, Sep. 2014.

[2] D. L. Pauls, A. Abramovitch, S. L. Rauch, and D. A. Geller, "Obsessive-compulsive disorder: An integrative genetic and neurobiological perspective," *Nature Rev. Neurosci.*, vol. 15, no. 6, pp. 410–424, Jun. 2014.

[3] J. Posner, R. Marsh, T. V. Maia, B. S. Peterson, A. Gruber, and H. B. Simpson, "Reduced functional connectivity within the limbic cortico-striato-thalamo-cortical loop in unmedicated adults with obsessive-compulsive disorder," *Hum. Brain Mapping*, vol. 35, no. 6, pp. 2852–2860, Jun. 2014.

[4] Y. Sakai *et al.*, "Corticostriatal functional connectivity in non-medicated patients with obsessive-compulsive disorder," *Eur. Psychiatry*, vol. 26, no. 7, pp. 463–469, Oct. 2011.

[5] P. Li *et al.*, "Altered resting state functional connectivity patterns of the anterior prefrontal cortex in obsessive-compulsive disorder," *Neuroreport*, vol. 23, no. 11, pp. 681–686, Aug. 2012.

[6] T. Zhang, "Abnormal small-world architecture of top–down control networks in obsessive–compulsive disorder," *J. Psychiatry Neurosci.*, vol. 36, no. 1, pp. 23–31, Jan. 2011.

[7] W. H. Jung *et al.*, "Altered functional network architecture in orbitofronto-striato-thalamic circuit of unmedicated patients with obsessive-compulsive disorder," *Hum. Brain Mapping*, vol. 38, no. 1, pp. 109–119, Jan. 2017.

[8] Y. He *et al.*, "Uncovering intrinsic modular organization of spontaneous brain activity in humans," *PLoS ONE*, vol. 4, no. 4, p. e5226, Apr. 2009.

[9] L. Luo *et al.*, "Altered brain functional network dynamics in obsessive–compulsive disorder," *Hum. Brain Mapping*, vol. 42, no. 7, pp. 2061–2076, May 2021.

[10] J. Calzà *et al.*, "Altered cortico–striatal functional connectivity during resting state in obsessive–compulsive disorder," *Frontiers Psychiatry*, vol. 10, p. 319, May 2019.

[11] B. J. Harrison *et al.*, "Brain corticostriatal systems and the major clinical symptom dimensions of obsessive-compulsive disorder," *Biol. Psychiatry*, vol. 73, no. 4, pp. 321–328, Feb. 2013.

[12] D. H. Kang *et al.*, "Neural correlates of altered response inhibition and dysfunctional connectivity at rest in obsessive-compulsive disorder," *Prog. Neuro-Psychopharmacol Biol. Psychiatry*, vol. 40, pp. 340–346, Jan. 2013.

[13] A. Anticevic *et al.*, "Global resting-state functional magnetic resonance imaging analysis identifies frontal cortex, striatal, and cerebellar dysconnectivity in obsessive-compulsive disorder," *Biol. Psychiatry*, vol. 75, no. 8, pp. 595–605, Apr. 2014.

[14] J. A. Cardin *et al.*, "Driving fast-spiking cells induces gamma rhythm and controls sensory responses," *Nature*, vol. 459, no. 7247, pp. 663–667, Jun. 2009.

[15] Y. Tian, H. Zhou, H. Zhang, and T. Li, "Research on differential brain networks before and after WM training under different frequency band oscillations," *Neural Plasticity*, vol. 2021, Mar. 2021, Art. no. 6628021.

[16] M. Ischebeck, T. Endrass, D. Simon, and N. Kathmann, "Altered frontal EEG asymmetry in obsessive-compulsive disorder," *Psychophysiology*, vol. 51, no. 7, pp. 596–601, Jul. 2014.

[17] S. Velikova, M. Locatelli, C. Insacco, E. Smeraldi, G. Comi, and L. Leocani, "Dysfunctional brain circuitry in obsessive-compulsive disorder: Source and coherence analysis of EEG rhythms," *NeuroImage*, vol. 49, no. 1, pp. 977–983, Jan. 2010.

[18] J. Koprivova *et al.*, "EEG source analysis in obsessive-compulsive disorder," *Clin. Neurophysiol.*, vol. 122, no. 9, pp. 1735–1743, Sep. 2011.

[19] S. Olbrich, H. Olbrich, M. Adamaszek, I. Jahn, U. Hegerl, and K. Stengler, "Altered EEG lagged coherence during rest in obsessive-compulsive disorder," *Clin. Neurophysiol.*, vol. 124, no. 12, pp. 2421–2430, Dec. 2013.

[20] D. Kamaradova *et al.*, "Cognitive deficits in patients with obsessive–compulsive disorder–electroencephalography correlates," *Neuropsychiatric Disease Treat.*, vol. 12, pp. 1119–1125, May 2016.

[21] M. J. Koh *et al.*, "Altered resting-state functional connectivity in patients with obsessive–compulsive disorder: A magnetoencephalography study," *Int. J. Psychophysiol.*, vol. 123, pp. 80–87, Jan. 2018.

[22] Y. Dasdemir, E. Yildirim, and S. Yildirim, "Analysis of functional brain connections for positive–negative emotions using phase locking value," *Cognit. Neurodyn.*, vol. 11, no. 6, pp. 487–500, Dec. 2017.

[23] P. Xu *et al.*, "Different topological organization of human brain functional networks with eyes open versus eyes closed," *NeuroImage*, vol. 90, pp. 246–255, Apr. 2014.

[24] F. Miraglia, F. Vecchio, P. Bramanti, and P. M. Rossini, "EEG characteristics in 'eyes-open' versus 'eyes-closed' conditions: Small-world network architecture in healthy aging and age-related brain degeneration," *Clin. Neurophysiol.*, vol. 127, no. 2, pp. 1261–1268, Feb. 2016.

[25] F. Perrin, J. Pernier, O. Bertrand, and J. F. Echallier, "Spherical splines for scalp potential and current density mapping," (in eng), *Electroencephalography Clin. Neurophysiol.*, vol. 72, no. 2, pp. 184–187, Feb. 1989.

[26] B. Tan, X. Kong, P. Yang, Z. Jin, and L. Li, "The difference of brain functional connectivity between eyes-closed and eyes-open using graph theoretical analysis," *Comput. Math. Methods Med.*, vol. 2013, Oct. 2013, Art. no. 976365.

[27] A. K. Engel, P. Fries, and W. Singer, "Dynamic predictions: Oscillations and synchrony in top-down processing," (in eng), *Nature Rev. Neurosci.*, vol. 2, no. 10, pp. 704–716, Oct. 2001.

[28] J. P. Lachaux, E. Rodriguez, J. Martinerie, and F. J. Varela, "Measuring phase synchrony in brain signals," *Hum. Brain Mapping*, vol. 8, no. 4, pp. 194–208, Jan. 1999.

[29] J. Fell and N. Axmacher, "The role of phase synchronization in memory processes," *Nature Rev. Neurosci.*, vol. 12, no. 2, pp. 18–105, Feb. 2011.

[30] S. H. Strogatz, "Exploring complex networks," (in eng), *Nature*, vol. 410, no. 6825, pp. 268–276, Mar. 2001.

[31] D. J. Watts and S. H. Strogatz, "Collective dynamics of 'small-world' networks," (in eng), *Nature*, vol. 393, no. 6684, pp. 440–442, Jun. 1998.

[32] E. Bullmore and O. Sporns, "Complex brain networks: Graph theoretical analysis of structural and functional systems," *Nature Rev. Neurosci.*, vol. 10, pp. 98–186, Mar. 2009.

[33] S.-H. Jin, W. Jeong, J. Seol, J. Kwon, and C. K. Chung, "Functional cortical hubs in the eyes-closed resting human brain from an electrophysiological perspective using magnetoencephalography," *PLoS ONE*, vol. 8, no. 7, Jul. 2013, Art. no. e68192.

[34] A. Zalesky, A. Fornito, and E. T. Bullmore, "Network-based statistic: Identifying differences in brain networks," *NeuroImage*, vol. 53, no. 4, pp. 1197–1207, Dec. 2010.

[35] B. Erdeniz, E. Serin, Y. Ibadi, and C. Taş, "Decreased functional connectivity in schizophrenia: The relationship between social functioning, social cognition and graph theoretical network measures," *Psychiatry Res., Neuroimaging*, vol. 270, pp. 22–31, Dec. 2017.

[36] C.-H. Lai, Y.-T. Wu, and Y.-M. Hou, "Functional network-based statistics in depression: Theory of mind subnetwork and importance of parietal region," *J. Affect. Disorders*, vol. 217, pp. 132–137, Aug. 2017.

[37] M. Xia, J. Wang, and Y. He, "BrainNet viewer: A network visualization tool for human brain connectomics," *PLoS ONE*, vol. 8, no. 7, Jul. 2013, Art. no. e68910.

[38] D. J. Shin *et al.*, "The effects of pharmacological treatment on functional brain connectome in obsessive-compulsive disorder," *Biol Psychiatry*, vol. 75, no. 8, pp. 606–614, Apr. 2014.

[39] O. Sporns, "Graph theory methods: Applications in brain networks," *Dialogues Clin. Neurosci.*, vol. 20, no. 2, pp. 111–121, Jun. 2018.

[40] Z. Kaposzta, O. Stylianou, P. Mukli, A. Eke, and F. S. Racz, "Decreased connection density and modularity of functional brain networks during n-back working memory paradigm," *Brain Behav.*, vol. 11, no. 1, p. e01932, Jan. 2021.

[41] R. Cao *et al.*, "Hemispheric asymmetry of functional brain networks under different emotions using EEG data," *Entropy*, vol. 22, no. 9, p. 939, Aug. 2020.

[42] E. Olejarczyk and W. Jernajczyk, "Graph-based analysis of brain connectivity in schizophrenia," *PLoS ONE*, vol. 12, no. 11, Nov. 2017, Art. no. e0188629.

[43] Z. Zhong *et al.*, "Abnormal topological organization in white matter structural networks revealed by diffusion tensor tractography in unmedicated patients with obsessive–compulsive disorder," *Prog. Neuro-Psychopharmacol. Biol. Psychiatry*, vol. 51, pp. 39–50, Jun. 2014.

[44] V. Latora and M. Marchiori, "Efficient behavior of small-world networks," *Phys. Rev. Lett.*, vol. 87, Oct. 2001, Art. no. 198701.

[45] C. Zhou *et al.*, "Altered white matter structural networks in drug-naive patients with obsessive-compulsive disorder," *Brain Imag. Behav.*, vol. 15, no. 2, pp. 700–710, Apr. 2021.

[46] C. J. Stam, "Functional connectivity patterns of human magnetoencephalographic recordings: A 'small-world' network?" *Neurosci. Lett.*, vol. 355, nos. 1–2, pp. 8–25, Jan. 2004.

[47] B. Cheng *et al.*, "Abnormal dynamics of resting-state functional activity and couplings in postpartum depression with and without anxiety," *Cerebral Cortex*. Accessed: Feb. 17, 2022. [Online]. Available: https://doi.org/10.1093/cercor/bhac038

[48] T. C. Shi, D. Pagliaccio, M. Cyr, H. B. Simpson, and R. Marsh, "Network-based functional connectivity predicts response to exposure therapy in unmedicated adults with obsessive–compulsive disorder," *Neuropsychopharmacology*, vol. 46, no. 5, pp. 1035–1044, Apr. 2021.

[49] O. M. Bazanova and D. Vernon, "Interpreting EEG alpha activity," *Neurosci. Biobehavioral Rev.*, vol. 44, pp. 94–110, Jul. 2014.

[50] J. Y. Park, J. Lee, H.-J. Park, J.-J. Kim, K. Namkoong, and S. J. Kim, "Alpha amplitude and phase locking in obsessive-compulsive disorder during working memory," *Int. J. Psychophysiol.*, vol. 83, no. 1, pp. 1–7, Jan. 2012.

[51] Y. Zhang, Y. Chen, S. L. Bressler, and M. Ding, "Response preparation and inhibition: The role of the cortical sensorimotor beta rhythm," *Neuroscience*, vol. 156, no. 1, pp. 238–246, Sep. 2008.

[52] C. Jia *et al.*, "Decreased resting-state interhemispheric functional connectivity in medication-free obsessive-compulsive disorder," *Frontiers Psychiatry*, vol. 11, Sep. 2020, Art. no. 559729.

[53] E. Bullmore and O. Sporns, "The economy of brain network organization," *Nature Rev. Neurosci.*, vol. 13, no. 5, pp. 336–349, Apr. 2012.

[54] J. Sepulcre, H. Liu, T. Talukdar, I. Martincorena, B. T. T. Yeo, and R. L. Buckner, "The organization of local and distant functional connectivity in the human brain," *PLoS Comput. Biol.*, vol. 6, no. 6, Jun. 2010, Art. no. e1000808.

[55] A. E. Cave and R. J. Barry, "Sex differences in resting EEG in healthy young adults," *Int. J. Psychophysiol.*, vol. 161, pp. 35–43, Mar. 2021.

[56] M. Moosmann *et al.*, "Correlates of alpha rhythm in functional magnetic resonance imaging and near infrared spectroscopy," *NeuroImage*, vol. 20, no. 1, pp. 145–158, Sep. 2003.

[57] L. Wan *et al.*, "From eyes-closed to eyes-open: Role of cholinergic projections in EC-to-EO alpha reactivity revealed by combining EEG and MRI," *Hum. Brain Mapping*, vol. 40, no. 2, pp. 566–577, Feb. 2019.

[58] K. Hufner *et al.*, "Differential effects of eyes open or closed in darkness on brain activation patterns in blind subjects," *Neurosci. Lett.*, vol. 466, no. 1, pp. 4–30, Nov. 2009.

[59] J. Kayser and C. E. Tenke, "Principal components analysis of Laplacian waveforms as a generic method for identifying ERP generator patterns: I. Evaluation with auditory oddball tasks," *Clin. Neurophysiol.*, vol. 117, no. 2, pp. 348–368, Feb. 2006.